DESIGN OF OPTIMALLY SMOOTHING MULTISTAGE SCHEMES FOR THE EULER EQUATIONS

BRAM VAN LEER, WEN-TZONG LEE, PHILIP L. ROE AND KENNETH G. POWELL

Department of Aerospace Engineering, The University of Michigan, Ann Arbor, MI 48109-2140, U.S.A.

AND

CHANG-HSIEN TAI

Department of Mechanical Engineering, Chung Cheng Institute of Technology, Ta Shi, Tao Yuan, Taiwan, R.O.C.

SUMMARY

A recently derived local preconditioning of the Euler equations is shown to be useful in developing multistage schemes suited for multigrid use. The effect of the preconditioning matrix on the spatial Euler operator is to equalize the characteristic speeds. When applied to the discretized Euler equations, the preconditioning has the effect of strongly clustering the operator's eigenvalues in the complex plane. This makes possible the development of explicit marching schemes that effectively damp most high-frequency Fourier modes, as desired in multigrid applications. The technique is the same as developed earlier for scalar convection schemes: placement of the zeros of the amplification factor of the multistage scheme in locations where eigenvalues corresponding to high-frequency modes abound.

1. INTRODUCTION

Recently, Tai[1,2] presented and tested multistage schemes with optimized high-frequency damping, for the time integration of convection or convection–diffusion equations. These schemes are intended for use as a single-grid solver in a multigrid strategy, but they also render good service as robust single-grid time-marching schemes. The derivation is straightforward for one-dimensional convection and readily extends to two and three dimensions, provided that an appropriate effective mesh width in the direction of convection is defined. Tai's results have already been improved upon by Catalano and Deconinck.[3] The extension of the theory to a non-linear system of convection equations, such as the multidimensional Euler equations, so far has failed, because of the large spread of the characteristic speeds (the convection speeds hidden in the equations).

A local preconditioning technique, recently derived,[4] largely removes this spread. It achieves what can be shown to be the optimal condition number for the characteristic speeds, namely, $1/\sqrt{[1 - \min(M^2, M^{-2})]}$, where M is the local Mach number. This is a major improvement over the condition number before preconditioning, which equals $(M + 1)/\min(M, |M - 1|)$.

The purpose of this paper is to introduce the new preconditioning to the multigrid research community, and discuss its potential benefits for the multigrid computation of steady solutions of the Euler equations.

The effect of the preconditioning on discretizations of the spatial operator in the Euler equations is a strong concentration of the pattern of eigenvalues in the complex plane. This

now makes it possible to design multistage schemes that systematically damp most high-frequency waves admitted by the particular discrete operator, using the techniques in References 1 and 2. Such schemes will again be favourable single-grid solvers for use in a multigrid strategy; at the same time these are also superior explicit single-grid schemes, as the preconditioning makes the characteristic convection equations evolve at the same rate.

The use of a local preconditioning to overcome the large spread among characteristic speeds has so far been limited to the regime of almost incompressible flow ($M \to 0$); see Turkel,[5] and Feng and Merkle.[6] The present preconditioning is effective over the entire Mach-number range.

2. OPTIMIZATION OF HIGH-FREQUENCY DAMPING FOR CONVECTION SCHEMES

Tai's procedure[1] for optimizing the high-frequency damping in a one-dimensional convection scheme is a geometry exercise in the complex plane: putting the zeros of the multistage amplification factor on top of the locus of the Fourier transform – the 'Fourier footprint' – of the discrete spatial operator. This can be achieved for one specific value of the time step, the finding of which is part of the design process. An example of the result of this procedure is shown in Figure 1. Catalano and Deconinck[3] relaxed the condition that the zeros must lie exactly on the Fourier locus, thereby achieving a further reduction of the maximum amplification factor for the high frequencies.

For a two-dimensional discrete convection operator the Fourier footprint is no longer a single curve, but covers an area; the location and shape of this area vary greatly with the convection direction. Figure 2 shows the locus for the first-order upwind-differencing operator, for convection directions of $10°$ and $45°$. High-frequency damping by a fixed multistage scheme (coefficients independent of flow direction) is easily achieved for modes propagating in the physical convection direction, but is fundamentally difficult for modes varying in the
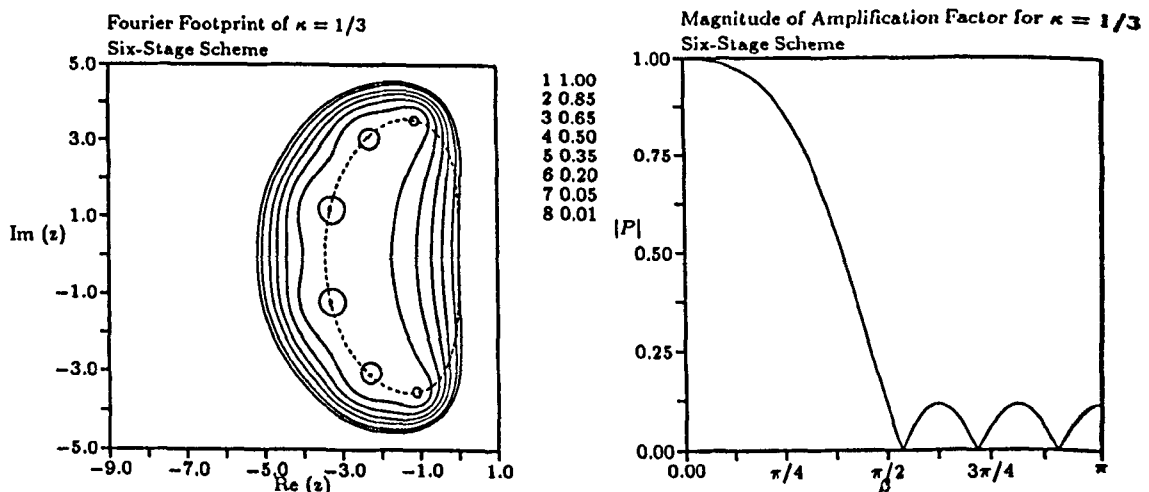

Figure 1. Left: Fourier footprint in the complex plane (broken line) of the third-order upwind-biased spatial discretization of the one-dimentional convection operator, and level lines (solid), up to the level 1, of the amplification factor of Tai's optimal six-stage scheme. The desired time step corresponds to a Courant number of $2 \cdot 5975$; right: modulus of the amplification factor as a function of spatial frequency

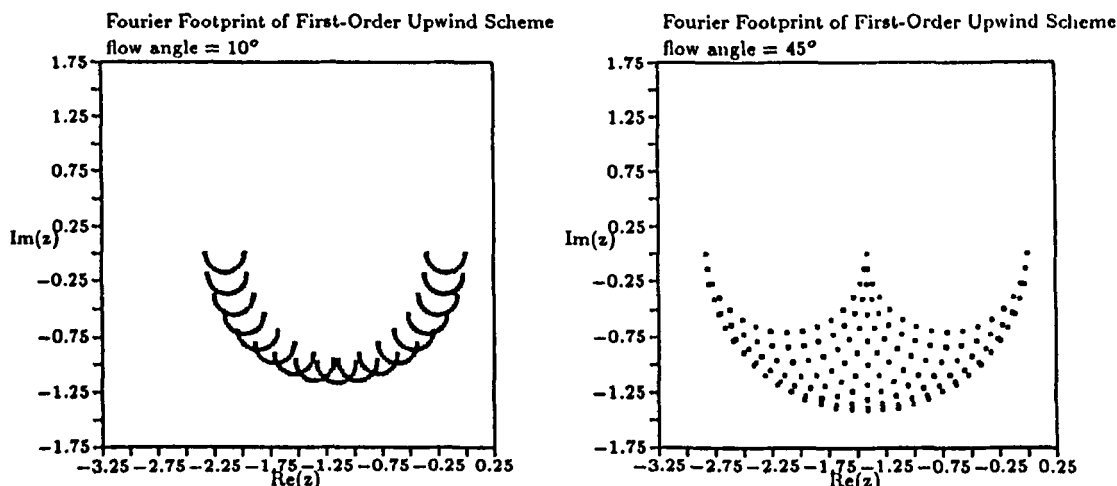Fourier Footprint of First-Order Upwind Scheme   Fourier Footprint of First-Order Upwind Scheme

Figure 2. Left: Fourier footprint in the complex plane of the first-order upwind approximation of the two-dimensional convection operator, for a convection speed at an angle of $10°$ with respect to the grid. The frequencies included in the footprint are $\beta_x \in [0, \pi]$, $\beta_y \in [0, \pi]$. The low–high frequency combinations are found close to the origin, making damping by a multistage scheme hard to achieve. The timestep chosen corresponds to a Courant number of 1; right: same for a convection speed at an angle of $45°$ with respect to the grid

normal direction, especially if the convection is almost in the grid direction, and the spatial discretization is of higher-order accuracy. This is what we may call the single-grid alignment problem; its solution lies beyond the scope of this paper.

The alignment problem is evident for a $10°$ angle from the low–high frequency combinations found near the origin. To damp these, zeros must be put close to the origin; to benefit from these zeros, a large time step would be needed; this works against numerical stability.

For the two-dimensional Euler equations the situation becomes even worse, because there are now different kinds of physical signals propagating in all possible directions at different speeds; these are approximately represented by the discrete operator and produce different concentrations of eigenvalues in its Fourier footprint. Figure 3 shows the Fourier footprint of the first-order upwind scheme for the Euler equations, based on Roe's[7] upwind-biased flux formula, for a range of Mach numbers. All graphs are for the case when the flow speed is aligned with the grid. The variable dimensions of the different concentrations in the footprint make it impossible to place the zeros of a multistage amplification factor at fixed locations in the complex plane and still achieve good high-frequency damping for all Mach numbers (even disregarding the flow angle).

3. LOCAL PRECONDITIONING OF THE EULER EQUATIONS

The two-dimensional Euler equations can be written as

$$\frac{\partial U}{\partial t} - A(U) \frac{\partial U}{\partial x} - B(U) \frac{\partial U}{\partial y} = \text{Res}(U) \tag{1}$$

For simplicity of notation we may assume that the flow is aligned with the positive x-direction, and that the state vector U includes as its components pressure p (suitably normalized), two velocities u and v, and entropy (expressed in terms of pressure and density ρ; a denotes the

Fourier Footprint of First-Order Roe Scheme
local dt, M=0.1, flow angle = 0°, CFL=1

Fourier Footprint of First-Order Roe Scheme
local dt, M=0.5, flow angle = 0°, CFL=1

Fourier Footprint of First-Order Roe Scheme
local dt, M=0.9, flow angle = 0°, CFL=1

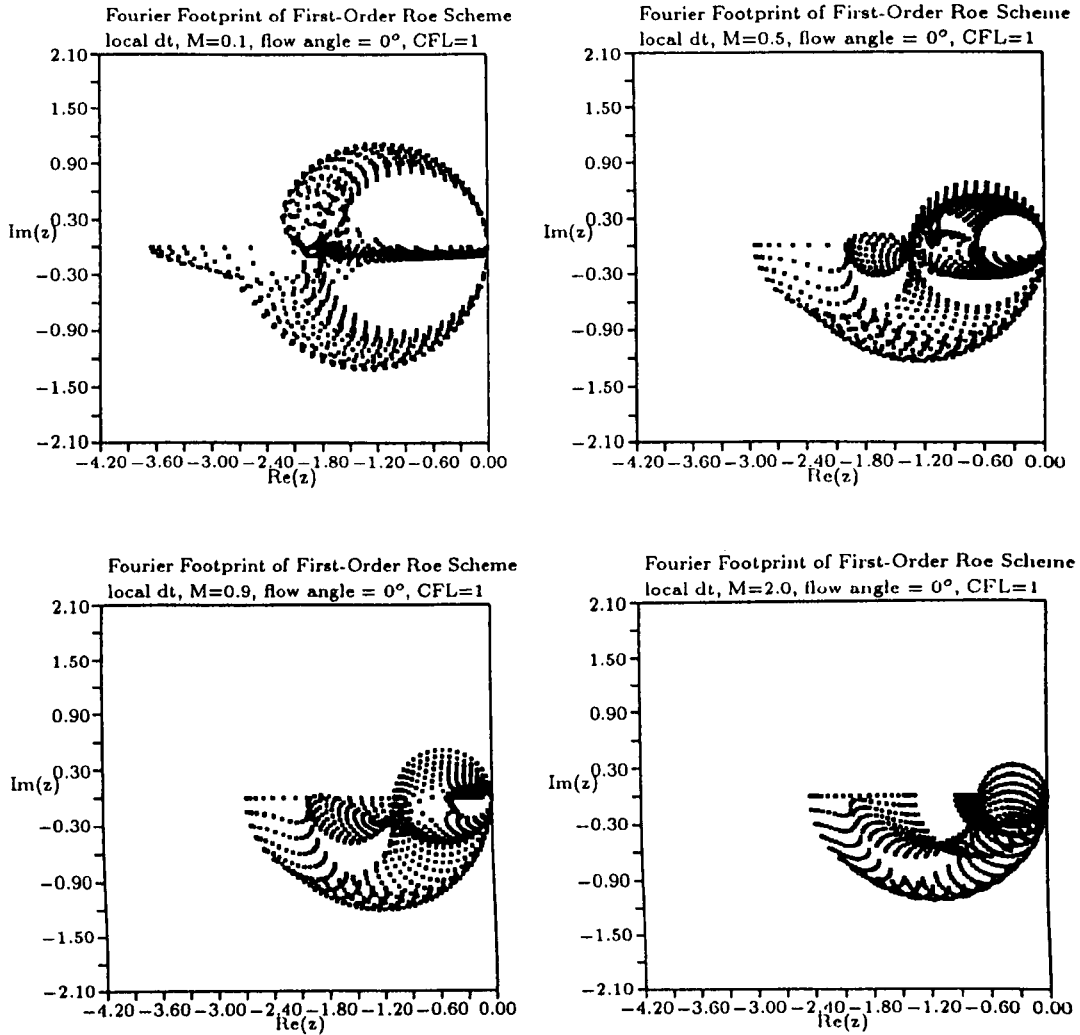Fourier Footprint of First-Order Roe Scheme
local dt, M=2.0, flow angle = 0°, CFL=1

Figure 3. Fourier footprint in the complex plane of the first-order upwind approximation of the spatial Euler operator, for $M = 0\cdot1$, $0\cdot5$, $0\cdot9$ and $2\cdot0$, and flow speed aligned with the grid. The frequencies included in the footprint are $\beta_x \in [0, \pi]$, $\beta_y \in [0, \pi]$. The timestep chosen corresponds to a Courant number of 1

speed of sound):

$$dU = \begin{pmatrix} \dfrac{dp}{\rho a} \\ du \\ dv \\ dp - a^2 d\rho \end{pmatrix}, \quad A = \begin{pmatrix} u & a & 0 & 0 \\ a & u & 0 & 0 \\ 0 & 0 & u & 0 \\ 0 & 0 & 0 & u \end{pmatrix}, \quad B = \begin{pmatrix} 0 & 0 & a & 0 \\ 0 & 0 & 0 & 0 \\ a & 0 & 0 & 0 \\ 0 & 0 & 0 & 0 \end{pmatrix} \tag{2}$$

The preconditioning matrix **P** derived in Reference 4 is thought to multiply the right-hand side of equation (1):

$$\frac{\partial U}{\partial t} = - PA \frac{\partial U}{\partial x} - PB \frac{\partial U}{\partial y} \tag{3}$$

It has the form

$$\mathbf{P_{2D}} = \begin{bmatrix} \dfrac{\tau}{\beta^2}M^2 & -\dfrac{\tau}{\beta^2}M & 0 & 0 \\[2mm] -\dfrac{\tau}{\beta^2}M & \dfrac{\tau}{\beta^2}+1 & 0 & 0 \\[2mm] 0 & 0 & \tau & 0 \\[2mm] 0 & 0 & 0 & 1 \end{bmatrix}, \; \beta = \sqrt{(|1-M^2|)}, \; \tau = \sqrt{[1-\min(M^2, M^{-2})]} \quad (4)$$

The wave-propagation properties of the preconditioned Euler equations differ substantially from those of the regular Euler equations. This is illustrated in Figure 4. The left frame shows, among other things, how a point-disturbance propagates according to the Euler equations for $M = u/a = 0\cdot5$. Entropy and shear components move with the flow, i.e. in the x-direction at speed $0\cdot5$, while an acoustic front spreads relative to the fluid at speed 1. The largest ratio between two wave speeds in this diagram, i.e. the condition number, is found between the forward acoustic signal in the x-direction and either the backward acoustic signal or the flow speed; it equals 3.

The right frame shows that after preconditioning the differences among the wave speeds are almost gone: the acoustic front is no longer centred on the moving fluid but at the origin of the point disturbance. Its shape has become an ellipse, with axes $\frac{1}{2}\sqrt{3}$ and 1; the flow speed also equals 1. The new condition number therefore is $2/\sqrt{3} = 1\cdot15$. Larger reductions of the condition number occur for Mach numbers near 0 or 1.

The above preconditioning has been extended to the three-dimensional Euler equations.[4]

4. NUMERICAL IMPLEMENTATION OF PRECONDITIONING

An essential question is: how will the preconditioning, designed for the partial differential equations, act upon the discretized equations, i.e. in the presence of a numerical truncation error?

Initial numerical experiments, in which the preconditioning was applied to a standard first-order upwind-differencing Euler scheme based on Roe's[7] flux function, indicated a severe stability restriction on the time step. Analysis showed that this restriction could be lifted only through a modification of the numerical flux function. The bottom line is that the *preconditioned* scheme must have the form of a first-order upwind-differencing scheme for the *preconditioned* Euler equations. For Roe's flux function the modification amounts to a subtle change in the artifical-dissipation matrix.[4] It turns out that the new matrix preconditioning does not always necessitate such a modification; for instance, no change was needed in an upwind-biased flux based on Van Leer's[8] flux-vector splitting. The same tolerance is expected of flux functions incorporating a scalar dissipation coefficient, such as used in central-differencing schemes.[9]

Figure 5 shows how preconditioning can speed up convergence to a steady solution for a single-grid scheme. The residual histories are shown for computations of the steady flow about a NACA 0012 aerofoil at $M_\infty = 0\cdot85$ and an angle of attack of $1\cdot0°$, on a 32×16 O-grid. Roe's flux function was used; the solution obtained with the preconditioned scheme is shown on the left. It includes transonic regions terminated by a shock on both sides of the aerofoil. The condition number in the far field equals $(1+0\cdot85)/(1-0\cdot85) = 12\cdot3$; preconditioning reduces this to $1/\sqrt{(1-0\cdot85^2)} = 1\cdot9$, a reduction by a factor $6\cdot5$. The convergence rate, after initial transients are gone, shows an increase of a factor $5\cdot5$.

The discussion and figures in the following Section are all based on the upwind scheme incorporating the modified flux function.

WAVE SPEEDS AND FRONT. 2-D EULER
M = 0.5 , no preconditioning

WAVE SPEEDS AND FRONT, 2-D EULER
M = 0.5, full preconditioning

___ 1st wave s
. . 1st wave f
___ 2nd wave s
▲ ▲ 2nd wave f
.... 3rd wave s
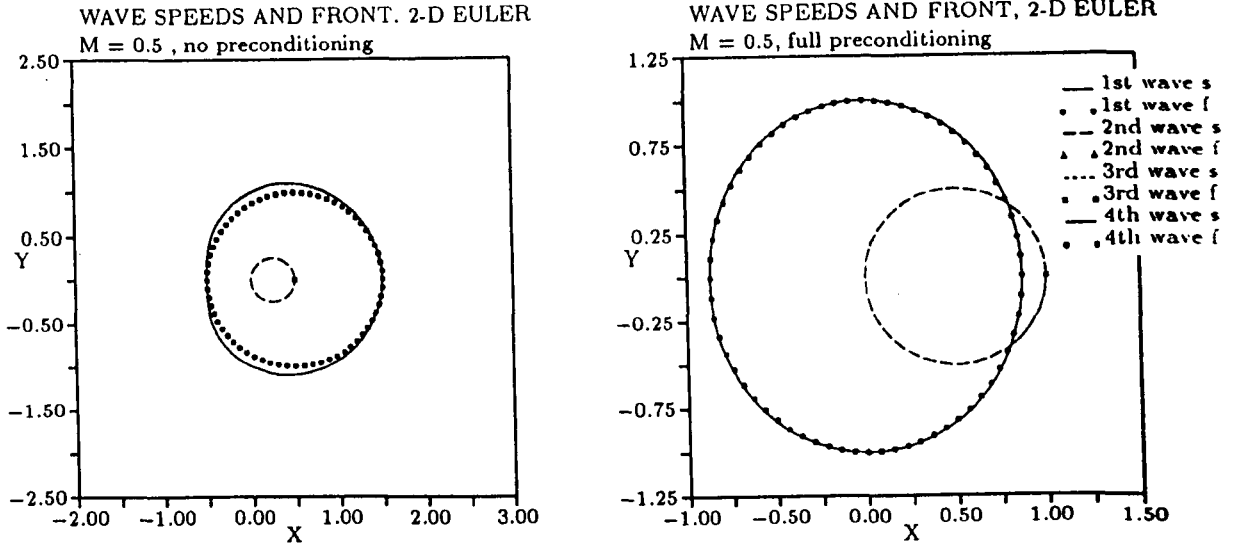. . 3rd wave f
___ 4th wave s
. . 4th wave f

Figure 4. Left: polar plot of plane-wave speeds (lines) and their envelopes (symbols) for $M = 0.5$, for the original Euler equations. The speeds of plane waves ('s' in legend) moving at an angle θ are the eigenvalues of $\mathbf{A} \cos \theta + \mathbf{B} \sin \theta$; the envelopes represent the wave fronts ('f' in legend) produced by a point disturbance. Waves 1 and 4 are sound waves, 2 is an entropy wave, and 3 is a shear wave; right: same for the preconditioned Euler equations
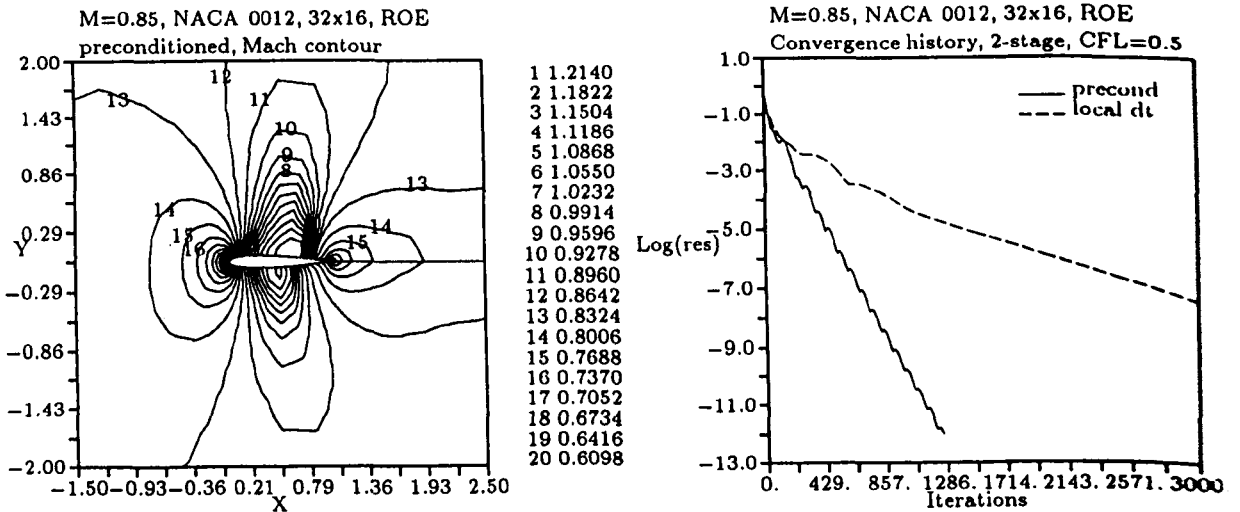
M=0.85, NACA 0012, 32x16, ROE
preconditioned, Mach contour

1	1.2140
2	1.1822
3	1.1504
4	1.1186
5	1.0868
6	1.0550
7	1.0232
8	0.9914
9	0.9596
10	0.9278
11	0.8960
12	0.8642
13	0.8324
14	0.8006
15	0.7688
16	0.7370
17	0.7052
18	0.6734
19	0.6416
20	0.6098

M=0.85, NACA 0012, 32x16, ROE
Convergence history, 2-stage, CFL=0.5

___ precond
--- local dt

Figure 5. Left: steady solution of the Euler equations for flow over a NACA 0012 aerofoil at $M_\infty = 0.85$, $\alpha = 1.0°$; Mach-number contours are shown. Matrix preconditioning was applied in combination with local time-stepping; right: residual-convergence histories for the computation of the solution at left (solid line) and a similar computation without preconditioning (broken line)

5. OPTIMIZATION OF HIGH-FREQUENCY DAMPING FOR THE PRECONDITIONED EULER EQUATION

The sequence of frames in Figure 6 shows the Fourier footprint of the preconditioned first-order upwind scheme for the Euler equations, again based on Roe's flux formula, for a range of Mach numbers. A comparison with the corresponding graphs in Section 2 shows that removing the variation among the characteristic convection speeds has resulted in a thorough clean-up of the footprint. Especially impressive is the job it does for small M. For $M \uparrow 1$ a growing separation of two regions of concentration of eigenvalues is observed; this
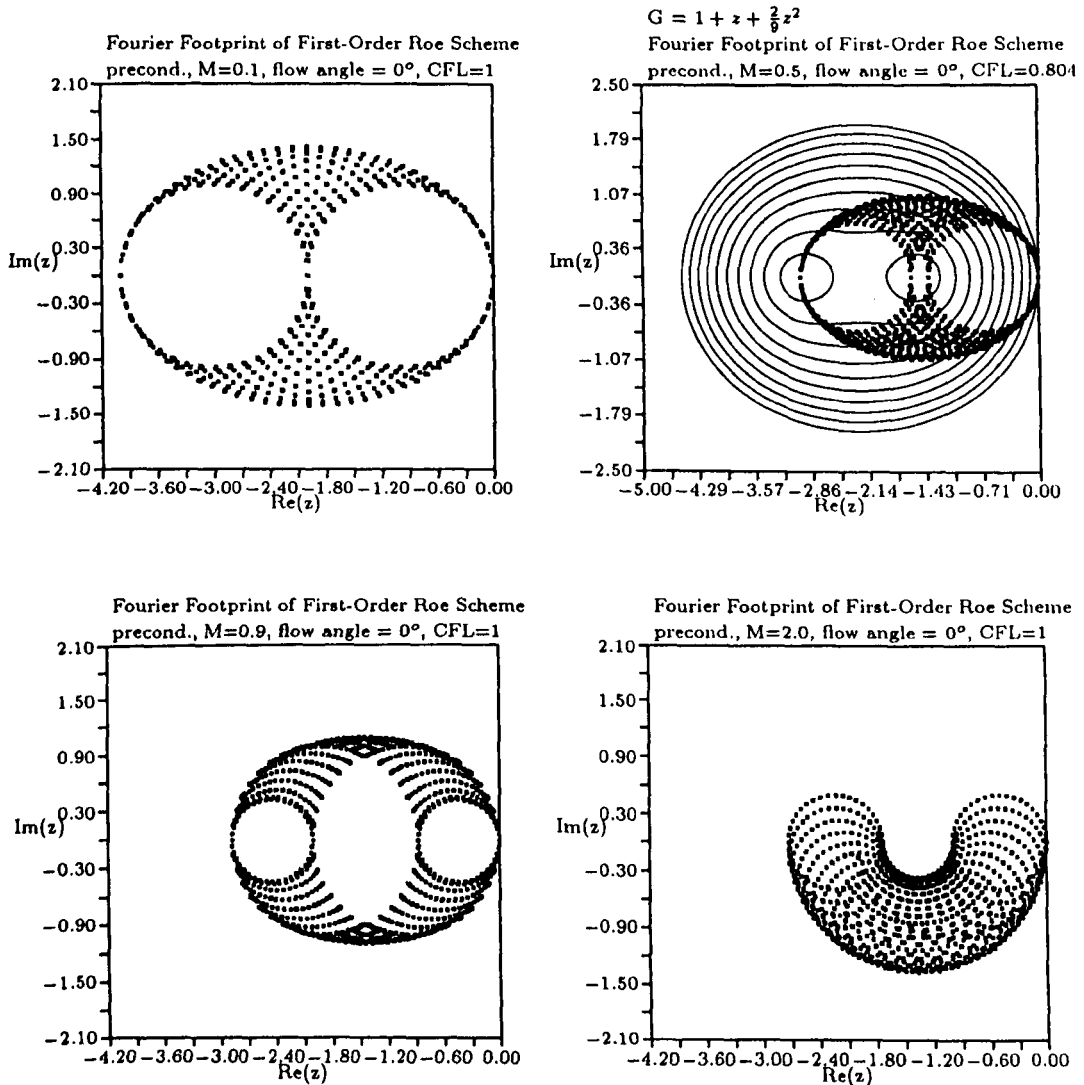

Figure 6. Fourier footprint in the complex plane of the preconditioned first-order upwind approximation of the spatial Euler operator, for $M = 0 \cdot 1$, $0 \cdot 5$, $0 \cdot 9$ and $2 \cdot 0$, and flow speed aligned with the grid. The frequenies included in the footprint are $\beta_x \in [0, \pi]$, $\beta_y \in [0, \pi]$. The timestep chosen corresponds to a Courant number of 1, except for $M = 0 \cdot 5$ (top-right frame), where it equals $0 \cdot 804$. This frame also shows level lines (solid), up to the level 1, of the amplification factor of a particular two-stage scheme (see main text)

corresponds to the growing disparity between the acoustic speeds in the flow direction $(= \sqrt{[1 - M^2]})$ and normal direction $(= 1)$. For $M > 1$ the footprint starts looking very much like one for scalar convection (cf. Figure 2); this is because all signals in supersonic flow move downstream. For $M = 0\cdot5$ (top-right frame) we have indicated the stability region associated with the two-stage method

$$\tilde{U} = U^n + \tfrac{2}{9}\Delta t \mathbf{Res}(U^n) \tag{5}$$

$$U^{n+1} = U^n + \Delta t \mathbf{Res}(\tilde{U}) \tag{6}$$

The amplification method associated with this method is the polynomial

$$P_2(z) = 1 + z + \tfrac{2}{9}z^2 = \left(1 + \frac{2z}{3}\right)\left(1 + \frac{z}{3}\right) \tag{7}$$

The zero of this polynomial at $z = -3$ can be placed on the location in the Fourier footprint where the highest frequencies occur ($\beta_x = \beta_y = \pi$), by choosing the appropriate time-step value; at the same time the other zero, at $z = -\tfrac{3}{2}$, falls in between the locations of the high–low ($\beta_x = \pi$, $\beta_y = 0$) and low–high ($\beta_x = 0, \beta_y = \pi$) frequency combinations, for any value of $M < 1$. This results in close-to-optimal short-wave damping for a two-stage scheme.

To illustrate this more clearly we show in Figure 7, for $M = 0\cdot5$, only those parts of the Fourier footprint that correspond to low–high (left) and high–low (right) and combinations of spatial frequencies in the x- and y-directions. Evident in the low–high frequency plot is the grid-alignment problem: there is a single arc extending from the origin, representing entropy and shear disturbances with low frequency in the x-direction – also the convection direction – and high frequency in the y-direction. Damping of these modes by a multistage method is impossible.

The above two-stage scheme is useful for grid-aligned flow, but is unstable when the flow angle differs too much from $0°$. It merely serves to illustrate the technique of optimizing high-
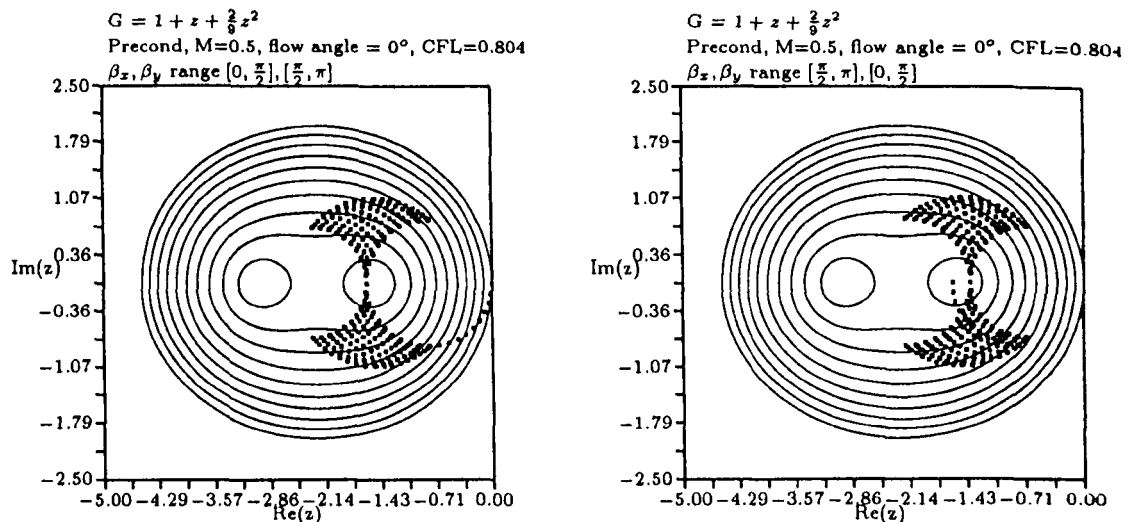

Figure 7. Partial Fourier footprint (symbols) for $M = 0\cdot5$, and level lines (solid) of the amplification factor of a two-stage scheme (see main text). Courant number $0\cdot804$. Left: low–high frequency combinations, $\beta_x \in [0, \pi/2]$, $\beta_y \in [\pi/2, \pi]$; right: high–low frequency combinations, $\beta_x \in [\pi/2, \pi]$, $\beta_y \in [0, \pi/2]$

frequency damping for an Euler scheme. Stability for all flow directions, combined with good high-frequency damping, requires at least a three-stage scheme.

It is clear from the level lines of $|P_2(z)|$ that there will be substantial high-frequency damping of acoustic modes for subsonic flow, specifically, for Mach numbers less than, but not too close to, 1. Damping of all acoustic modes for $M \uparrow 1$ remains problematic, as the vanishing acoustic speed in the x-direction causes the high–low frequency combinations to move toward the origin, although much more slowly than for the non-preconditioned scheme.

For supersonic flow the numerical properties of the spatial operator, preconditioned or not, more and more resemble those of a scalar convection operator, as the Mach number increases. The grid-alighment problem dominates; full high-frequency damping will have to come from other techniques than smart placement of zeros in the complex plane.

6. CONCLUSIONS

A recently derived local preconditioning of the Euler equations makes it possible to develop multistage schemes suited for multigrid use. The effect of the preconditioning matrix on the spatial Euler operator is to equalize the characteristic speeds. In numerical applications it has the effect of clustering the eigenvalues of finite-differencing operators approximating the spatial Euler operator. Owing to this clustering one can design multistage marching schemes that effectively damp most high-freuqency numerical error modes, as is desirable in multigrid applications.

One problem not solved by the preconditioning is: how to damp the combination of an error of high frequency in the normal direction coupled to a low frequency in the flow direction, when the flow is almost aligned with the grid.

REFERENCES

1. B. van Leer, C.-H. Tai and K. G. Powell, 'Design of optimally-smoothing multi-stage schemes for the Euler equations', in *AIAA 9th Computaitonal Fluid Dynamics Conference*, 1989.
2. C.-H. Tai, 'Acceleration techniques for explicit Euler codes', Ph.D. thesis, University of Michigan, 1990.
3. L. A. Catalano and H. Deconinck, 'Two-dimensional optimization of smoothing properties of multi-stage schemes applied to hyperbolic equations', in *Proceedings of the Third European Conference on Multigrid Methods*, 1990.
4. B. van Leer, W.-T. Lee and P. L. Roe, 'Characteristic time-stepping or local preconditioning of the Euler equations', in *AIAA 10th Computational Fluid Dynamics Conference*, 1991.
5. E. Turkel, 'Preconditioned methods for solving the incompressile and low speed compressible equations', *J. Comput. Phys.*, **72** (1987).
6. J. Feng and C. L. Merkle, 'Evaluation of preconditioning methods for time-marching systems', AIAA Paper 90-0016, 1990.
7. P. L. Roe, 'Characteristic-based schemes for the Euler equations', *Ann. Rev. Fluid Mech.*, **18**, 337–365 (1986).
8. B. van Leer, 'Flux-vector splitting for the Euler equations', *Lecture Notes in Physics*, **170** (1982).
9. A. Jameson, W. Schmidt and E. Turkel, 'Numerical solutions of the Euler equations by a finite-volume method using Runge-Kutta time-stepping schemes', AIAA Paper 81-1259, 1981.